Effects of Enzyme Inhibitors and Insulin Concentration on Transepithelial Transport of Insulin in Rats

JANE P. F. BAI AND L. L. CHANG

Department of Pharmaceutics, College of Pharmacy, University of Minnesota, Minneapolis, MN 55455, USA

Abstract

The objective of this study was to determine whether transepithelial transport of insulin can be improved by enzyme inhibitors and whether insulin concentration affects its ileal absorption.

Ussing chambers and radioimmunoassay were used to study insulin transport across the rat ileum, and circular dichroic spectra were used to determine whether insulin aggregated at high concentrations. Inhibitors that inhibit insulin-degrading enzyme, including N-ethylmaleimide, 1,10-phenanthroline and p-chloromercuribenzoate, dramatically improved insulin transport across the ileum. At 100 nm, the ileal permeability of immunoreactive insulin was 10^{-6} cm s^{-1} in the presence of inhibitors, and was negligible when inhibitors were not used. Ammonium chloride, a lysosomotropic agent that increases intralysosomal pH, and aprotinin, a proteasome inhibitor, did not increase transport of insulin to a detectable extent. Insulin permeability decreased as its concentration increased from 100 nm to 83·3 μM, and at 83·3 μM insulin aggregated.

It is concluded that insulin transport is improved by enzyme inhibitors, but is impaired by insulin aggregation at high concentrations.

Biochemical and morpho-cytochemical evidence has revealed that insulin is mainly absorbed transcellularly through the ileum, duodenum and colon in normal and diabetic rats (Bendayan et al 1990, 1994). Using the adenocarcinoma cell line HT-29 derived from human colon, insulin was also shown to be absorbed by receptor-mediated endocytosis (Sonne 1985). Insulin was, furthermore, shown to be mainly degraded by insulin-degrading enzyme (IDE) in small intestinal mucosal cell homogenate (Chang & Bai 1994; Bai & Chang 1995). If insulin degradation in the epithelium is rapid and follows first-order kinetics, its apparent permeability, P_{app}, derived from the continuity equation with appropriate boundary conditions considering an aqueous layer adjacent to the membrane (equation 1), is expressed in equation 2.

$$\frac{\delta C}{\delta t} = D_m \frac{\delta^2 C}{\delta z^2} - k_1 C = 0 \quad \text{at steady state} \quad (1)$$

$$P_{app} = \frac{P_a \left(\frac{P_c (k_1 D_m)^{1/2}}{\tan h(k_1 h_m/D_m)^{1/2}} \right)}{P_a + \left(\frac{P_c (k_1 D_m)^{1/2}}{\tan h(k_1 h_m/D_m)^{1/2}} \right)} \quad (2)$$

Where C is the insulin concentration in the epithelial membrane, P_{app} is the apparent permeability, k_1 is the first-order degradation rate constant, P_a is the aqueous permeability, P_c is the membrane/water insulin concentration ratio, which is highly influenced by the efficiency of receptor-mediated or fluid-phase endocytosis and insulin concentration, D_m is the diffusion coefficient of insulin in the membrane, and h_m is the membrane thickness. When degradation by epithelial enzymes is rapid, i.e., k_1 is large, P_{app} approaches zero. Conceivably, the number of insulin molecules surviving cellular enzymatic degradation will increase with concentration; at high con-

centrations, however, insulin forms large aggregates likely to result in low permeability. Because insulin-degrading enzyme (IDE) has been identified as the key enzyme degrading insulin in intestinal mucosal cell homogenate (Chang & Bai 1994; Bai & Chang 1995), this study was designed to determine insulin permeability in the presence of enzyme inhibitors and to understand how insulin concentration influences its absorption.

Methods

Bovine serum albumin, aprotinin, trichloroacetic acid, pentobarbital, 1,10-phenanthroline, N-ethylmaleimide, p-chloromercuribenzoate, PhAsO (phenylarsine oxide), and aprotinin were obtained from Sigma (St Louis, MO, USA). Insulin radioimmunoassay (RIA) kit was obtained from Diagnostic Products (Los Angeles, CA, USA). Zinc-free human recombinant insulin was a gift from Dr John Wang (Scios Nova, CA, USA). All other chemical reagents and buffer components were of analytical grade. All chemicals were used as obtained.

Male Sprague–Dawley rats, 250–300 g, were used as the animal model. Ussing chambers with a voltage clamp, borrowed from Dr Stephen Berge (3M Pharmaceuticals, St Paul, MN, USA), were used to study in-vitro ileal insulin permeability (Donowitz & Asarkof 1982; Quadros et al 1994). After removal of the serosa and muscularis propris, mucosal sheets were mounted on the Ussing chambers in the non-short-circuited state at 37°C and oxygenated with 95% oxygen–5% carbon dioxide. Krebs buffer solution of pH 7·4 was used to prepare insulin solution of 100 nM or higher concentrations. In the experimental groups insulin was added with an enzyme inhibitor to the mucosal chamber (donor chamber) whereas buffer with the same inhibitor was added to the serosal chamber (receiver chamber). In some experiments an enzyme inhibitor was added to the donor chamber only. In the control groups, no inhibitor was used. Samples were obtained from both serosal and mucosal chambers periodically.

Correspondence: J. P. F. Bai, Department of Pharmaceutics, College of Pharmacy, University of Minnesota, Minneapolis, MN 55455, USA.

Determination of transepithelial potential difference (mV) and short-circuit current (I) was used to assess tissue viability throughout the experiments. The initial resistance of ileal tissues was 50·6 ohm cm² which is similar to literature values (Kim et al 1994). In the control and experimental groups, the radioactivity of [³H]-D-glucose in the receiver chambers increased with time as 10 mM D-glucose and a trace amount of [³H]-D-glucose were initially added to both donor and receiver chambers. Insulin was assayed using a commercial RIA kit with a detection limit of 2 μU mL⁻¹. Steady-state flux, J, was determined from the linear regression of the amount transported-time profile, and membrane permeability was determined from $J = P(C_d - C_r)$ where C_d and C_r are, respectively, the donor and receiver concentrations of insulin. Throughout the course of experiment, the donor concentration of insulin remained constant in the presence of an IDE inhibitor, yet without an IDE inhibitor it declined dramatically at 100 nM and decreased slowly at 16·7 μM or 83·3 μM. HPLC analysis of the insulin concentration in the donor chambers was performed using an SIL autoinjector, an LC-600 pump, an SPD-6A UV spectrophotometric detector and a CR 601 recorder (Shimadzu, Kyoto, Japan). All analyses were performed with a C_{18} column (10 μM; 4·6 mm × 15 cm, 300 Å) from Vydac (Hesperia, CA, USA). The mobile phase was 0·05% trifluoroacetic acid in water-acetonitrile, 85 : 25. Insulin eluted at 6 min.

Circular dichroic spectra were determined using a CD spectropolarimeter (Jasco Model J710, Japan Spectroscopic, Tokyo, Japan) with temperature controlled at 37°C; 10- and 5-mm pathlength quartz cuvettes (American Scientific Products, McGaw Park, IL, USA) were used for the high- and low-wavelength regions, respectively. Krebs buffer was used to prepare 0·1 mg mL⁻¹ and 0·5 mg mL⁻¹ zinc-free insulin and 0·5 mg mL⁻¹ zinc-insulin. Molar ellipticities were calculated using the equation $[\theta]\lambda = \theta\lambda/(C \times 1)$, where $\theta\lambda$ is the observed ellipicity at wavelength λ, 1 is the pathlength in decimeters, and C is the insulin concentration in decimoles.

Results

Because insulin forms aggregates at concentrations above 100 nm (Derewenda et al 1990), insulin permeability was studied at this concentration to ensure high assay accuracy. Several methods were used to determine whether, throughout the experiments, the membranes were intact; the observations are summarized in Table 1. Samples from the receiver chambers did not have any detectable insulin-degrading activity. It was concluded that the epithelia were intact, and that the possibility of enzyme leakage causing the donor insulin level of the control group to decline was unlikely. The decrease of donor insulin concentration in the control group was probably caused by degradation by the brush-border membrane. In separate studies it was found that insulin was degraded by the intestinal brush-border and basolateral membranes, though at much lower rates than by cytosol, and that insulin-degrading enzyme was present in the brush-border membrane (data not shown). These observations are consistent with the report that insulin-degrading enzyme (IDE) was also present on the cell membrane (Duckworth 1988). In the control, ileal transport of insulin was negligible (Table 2). At the individual concentrations used (Table 2) the IDE inhibitors N-ethylmaleimide and P-chloromercuribenzoate achieved 100% inhibition of insulin

degradation by small intestinal mucosal homogenates whereas another IDE inhibitor, 1,10-phenanthroline, achieved only 70%. Considering that IDE contributed to the majority of cytosolic insulin degradation (Bai & Chang 1995); that IDE activity was also present in the cell membrane (Duckworth 1988); that IDE inhibitors N-ethylmaleimide and 1,10-phenanthroline extensively inhibited insulin degradation by ileal brush-border and basolateral membranes (data not shown); and that IDE inhibitors extensively inhibited insulin degradation by mucosal homogenate, insulin permeability was determined when its metabolism was controlled by these inhibitors.

When an IDE inhibitor such as N-ethylmaleimide or 1,10-phenanthroline or p-chloromercuribenzoate (Roth et al 1985; Duckworth 1988) was placed with insulin in both donor and receiver chambers, ileal insulin transport was dramatically improved (Table 2). N-ethylmaleimide achieved the highest permeability, followed by 1,10-phenanthroline, and then by p-chloromercuribenzoate. N-ethylmaleimide dramatically improved insulin transport, irrespective of whether it was added to both donor and receiver chambers (Table 2) or to the donor chamber only (permeability, $P = 10 \pm 0.3 \times 10^{-6}$ cm s⁻¹). When placed in the donor chambers only, 1,10-phenanthroline achieved smaller insulin permeability ($P = 3 \pm 1 \times 10^{-6}$ cm s⁻¹), with correlation coefficients less than 0·9 for the linear regression of the amount of insulin transported against time. When 1,10-phenanthroline was placed in both chambers or when N-ethylmaleimide was placed either in one chamber only or in both chambers, the correlation coefficients of linear regression were greater than 0·90.

The question of N-ethylmaleimide damaging the epithelium and thus causing artificial higher insulin permeability was answered by several observations, as listed in Table 3. Transport of D-glucose and PEG-4000 was not affected by N-ethylmaleimide. Further, no detectable activity of lactate dehydrogenase was observed in both donor and receiver chambers when N-ethylmaleimide was used. Although in the presence of N-ethylmaleimide the transepithelial electrical resistance (TEER) decreased to 20 ohm cm² approximately 120 min after the experiment began, this inhibitor only enhanced the permeability of phenol red 2·3 times; it enhanced insulin flux at 100 nM or at 16·7 μM more than 10 times,

Table 1. Various methods used to determine the integrity of ileal epithelium.

Measurement	Result
Transepithelial electrical resistance	Remained constant throughout the course of the experiment
[³H]-D-glucose	Accumulated in the receiver chamber when an equal amount of [³H]-D-glucose (trace) and D-glucose were added to both donor and receiver chambers
Lactate dehydrogenase activity	Not detectable in donor and receiver chambers
Phenol red	Its permeability was 2–3 fold lower than the reported value (Schilling & Mitra 1990)

Table 2.   Effects of enzyme inhibitors on insulin permeability in the ileum.

Inhibitor	Permeability ($\times 10^{-6}$ cm s^{-1})	n
Control	~ 0	4
N-Ethylmaleimide (2 mM)	$7\cdot7 \pm 1\cdot3$	8
1,10-phenanthroline (1 mM)	$3\cdot4 \pm 1\cdot1$	5
Ammonium chloride (10 mM)	~ 0	3
Aprotinin (0·1 mg mL^{-1})	~ 0	3
p-Chloromercuribenzoate (0·1 mM)	$2\cdot9 \pm 0\cdot7$	3
EDTA (5 mM)	~ 0	3

Each inhibitor was added to both donor and receiver chambers. Mean ± s.e.; insulin concentration, 100 nM.

however (Table 3). Because phenol red is absorbed predominantly through paracellular pores (Shiga et al 1987; Schilling & Mitra 1990) and insulin (M.W. = 6000) is much larger than phenol red (M.W. = 354), enhancement of insulin permeability should at most equal that of phenol red if it is absorbed only through the paracellular route as phenol red. It was, moreover, noted that N-ethylmaleimide at 5 mM did not enhance colonic permeability of carboxyfluorescein, a nonabsorbable marker, but completely reversed the enhancing effects of oleic acid on carboxyfluorescein absorption (Murakami et al 1988). This, together with information in the literature, implies that the effects of N-ethylmaleimide on insulin transport are unlikely to be a result of its damaging the epithelial integrity. Although these measurements did not detect gross changes of the epithelium caused by N-ethylmaleimide, it might, however, have had some subtle influence on insulin transport. A much higher enhancement of insulin transport by N-ethylmaleimide does not support the notion that insulin is absorbed predominantly via the paracellular route. By use of an immunohistochemical method it has been shown that insulin was absorbed transcellularly, not paracellularly, in the intestine (Bendayan et al 1994). The uptake of insulin in hepatocytes and adipocytes is by specific facilitated mechanisms such as receptor-mediated endocytosis and fluid-phase endocytosis (Sonne 1988). It would be interesting to determine whether enterocytes absorb insulin through similar mechanisms.

EDTA (ethylenediaminetetraacetic acid), a paracellular enhancer, enhanced the permeability of phenol red to a similar extent as did N-ethylmaleimide (Table 3); it did not, however, enhance insulin transport to any detectable extent (Table 2). Although EDTA moderately inhibited cytosolic insulin degradation (Bai & Chang 1995), its negligible effect on

insulin transport was probably a result of its extensive ionization at the pH studied, because EDTA has four carboxylic acid groups and a pK$_a$ of 5·3. The lack of enhancement of insulin absorption by EDTA also suggests that paracellular transport might not occur for insulin. Sodium glycodeoxycholate at 15 mM completely abolished the TEER 30 min after the experiment began. The much smaller reduction in TEER caused by N-ethylmaleimide indicates, therefore, that this inhibitor did not behave like bile salts which elicit lipolysis of membrane lipids. The TEER values were close to those of the control group when either 1,10-phenanthroline or p-chloromercuribenzoate was used. N-ethylmaleimide at 1 mM inhibits insulin binding to its membrane receptor whereas 1,10-phenanthroline has no effect on insulin binding (Sonne & Gliemann 1983). Although it is unknown whether N-ethylmaleimide interferes with insulin binding to its receptor on enterocytes, it did dramatically increase ileal transport of insulin (Table 2).

Aprotinin, a strong inhibitor of cytosolic proteasome but a weak inhibitor of IDE (Arrigo et al 1988; Duckworth 1988; Tsuji & Kurachi 1989) only weakly inhibited cytosolic insulin degradation (Bai & Chang 1995). Aprotinin, a large molecule (M.W. = 6512), is unlikely to permeate the intestinal membrane. Altogether, its weak inhibition and poor permeation might have resulted in no improvement in insulin absorption (Table 2). Ammonium chloride, a lysosomotropic agent which increases intralysosomal pH when incubated with cells (Sonne & Gliemann 1983; Chiang & Dice 1988) had no effect on insulin transport (Table 2), suggesting that lysosomal enzymes are probably not involved in limiting insulin absorption. This result is consistent with previous observations that in insulin target cells lysosomal enzymes are not the primary enzymes responsible for insulin degradation (Sonne & Gliemann 1983).

Table 3.   Effects of enzyme inhibitors on ileal transport.

Inhibitor		Permeability ($\times 10^{-6}$ cm s^{-1})			
		Phenol red	Insulin	[^{14}C]-PEG-4000	[^{3}H]-D-glucose
N-ethylmaleimide (0 mM)		$3\cdot5 \pm 0\cdot4$	~ 0	~ 0	Accumulated in receiver chambers
N-ethylmaleimide (2 mM)		$6\cdot6 \pm 0\cdot5$	$7\cdot7 \pm 1\cdot3$	~ 0	Accumulated in receiver chambers
EDTA	(0 mM)	$3\cdot5 \pm 0\cdot4$	~ 0		
	(5 mM)	$6\cdot7 \pm 1\cdot8$	~ 0		

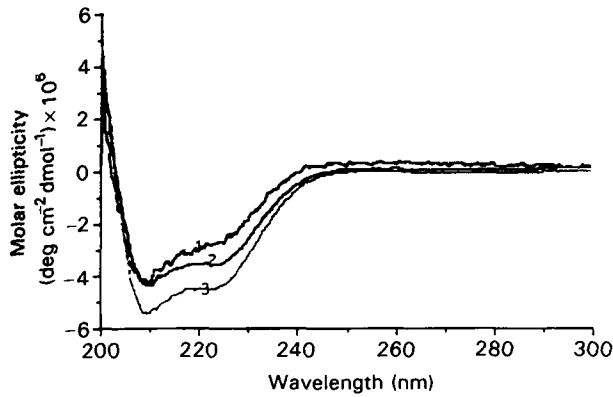Each inhibitor was added to both donor and receiver chambers. Mean ± s.e.; insulin concentration, 100 nM.

FIG. 1. The 200 nm to 300 nm circular dichroic spectra of insulin. A 5-mm pathlength quartz cuvette was used. 1. 0.1 mg mL^{-1} zinc-free insulin, 2. 0.5 mg mL^{-1} zinc-free insulin, 3. 0.5 mg mL^{-1} zinc-insulin.

To determine whether insulin formed aggregates in the experimental conditions used for the Ussing chambers studies, circular dichroic spectra of insulin were determined at various concentrations. Use of a 5-mm pathlength quartz cuvette resulted in two negative maxima, at 208 nm and 222 nm, for 0.1 mg mL^{-1} (16.7 μM) and 0.5 mg mL^{-1} (83.3 μM) zinc-free insulin and for 0.5 mg mL^{-1} zinc-insulin (Fig. 1). The 208-nm band is attributed to α-helix, a characteristic of the monomer involving residues B10-19, A2-6 and A13-19 (Goldman & Carpenter 1974), whereas the 222-nm band is
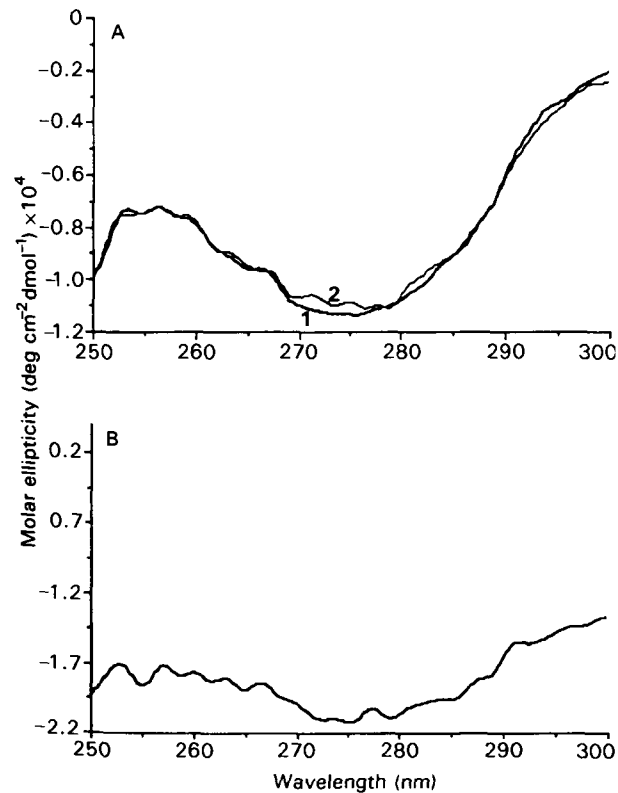

FIG. 2. The 250 nm to 300 nm circular dichroic spectra of insulin. A 10 mm pathlength quartz cuvette was used. A. 0.1 mg mL^{-1}, B. 0.5 mg mL^{-1}, 1. zinc-insulin, 2. zinc-free insulin.

attributed to an antiparallel β-structure, the main feature of the dimer (Goldman & Carpenter 1974). The negative maximum at 222 nm suggests that insulin dimers were formed in the Krebs buffer at both 0.1 and 0.5 mg mL^{-1}, and the negative maximum at 208 nm indicates that insulin monomers were also present. The negative maximum at 273 nm was not clear for 0.1 mg mL^{-1} and 0.5 mg mL^{-1} zinc-free insulin, and was only a minor band for 0.5 mg mL^{-1} zinc-insulin (Fig. 1). The negative maximum at 273 nm is attributed to optical activity associated with tyrosine and phenylalanine residues in the B23-28 region of the antiparallel β-structure formed between insulin monomers in the aggregates (Goldman & Carpenter 1974). Attenuation of this band is associated with insulin deaggregation.

When a 10-mm pathlength quartz cuvette was used to examine the near-ultraviolet circular dichroism spectrum (250–300 nm), there was a negative maximum at 273 nm for both zinc-free insulin and zinc-insulin at 0.5 mg mL^{-1}; at 0.1 mg mL^{-1}, however, the 273 nm band was not significant (Fig. 2) and it was, therefore, concluded that insulin formed dimers at 0.1 mg mL^{-1} (16.7 μM) and at 0.5 mg mL^{-1} (83.3 μM), and formed higher aggregates at 0.5 mg mL^{-1} but not at 0.1 mg mL^{-1}. Altogether, Figs 1 and 2 suggest that at 16.7 μM the zinc-free insulin solution contained monomers and dimers whereas at 83.3 μM it contained monomers, dimers and higher aggregates.

In the absence of N-ethylmaleimide, insulin transport was detectable at 16.7 μM and 83.3 μM but not at 100 nM, which suggests that at high concentrations more insulin molecules are able to survive epithelial degradation. In the presence of 1 mM or 2 mM N-ethylmaleimide, insulin permeability was calculable because the donor insulin concentration remained constant throughout the experiment. Insulin permeabilities at various concentrations are listed in Table 4. Interestingly, as insulin concentration increased 167-fold from 100 nM to 16.7 μM, its permeability remained similar, despite the formation of insulin dimers at 16.7 μM, as indicated in Figs 1 and 2. At 83.3 μM, insulin permeability was 15.4 times lower than that at 100 nM, and was 13 times lower than that at 16.7 μM. Insulin flux was concentration-dependent at concentrations below 100 nm (Fig. 3), but its increase was not proportional to concentration at concentrations above 100 nM, with the flux at 16.7 μM and 83.3 μM being 114-fold and 44-fold, respectively, that at 100 nM. Though it is unknown whether N-ethylmaleimide alters insulin aggregation, the less proportional increase of flux at 83.3 μM seemed to indicate that this inhibitor was unlikely to dissociate insulin aggregates.

Table 4. Effects of insulin concentration on its permeability ($\times 10^{-6}$ cm s^{-1}).

Concentration (μM)	Permeability
83.3	0.5 ± 0.2 (n = 5)
16.7*	6.5 ± 1.9 (n = 5)
100	7.7 ± 1.3 (n = 8)
50	3.7 ± 0.7 (n = 4)
25	6.1 ± 1.2 (n = 4)
1.3	4.5 ± 2.8 (n = 4)

Mean ± s.e.; 2 mM N-ethylmaleimide was added to both donor and receiver chambers except *1 mM N-ethylmaleimide.
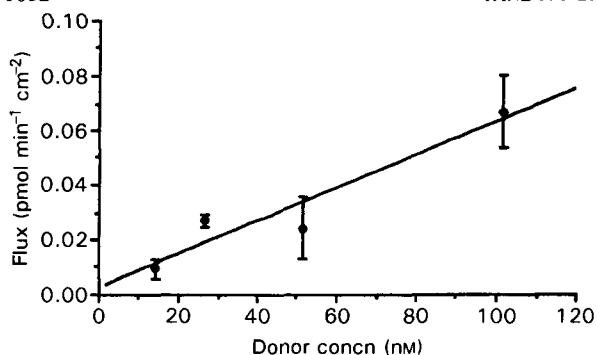
FIG. 3. The flux-concentration profile of insulin.

Interestingly, insulin absorption showed no lag time at 100 nM and 16·7 μM, but exhibited a lag time of 36 min at 83·3 μM (Fig. 4). No lag time at 16·7 μM and 100 nM seems to be in accordance with similar insulin permeabilities at both concentrations. It has been noted that insulin internalization became less efficient at concentrations higher than the physiological level (McClain & Olefsky 1988; Jochen et al 1989; Moss & Ward 1991) but it is unknown whether insulin internalization by enterocytes is also impaired at higher concentrations, resulting in a lag time at 83·3 μM.

Overall, the results suggest that intestinal absorption of insulin is improved by enzyme inhibitors, but is impaired by formation of insulin aggregates.
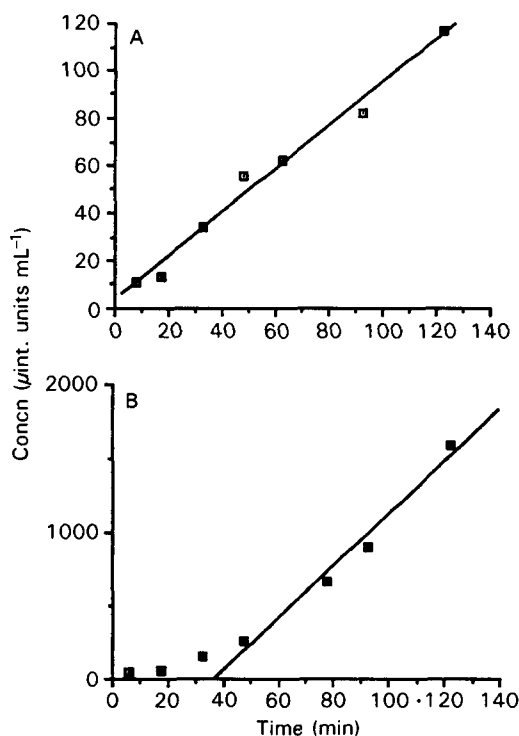

FIG. 4. The insulin concentration–time profile in the receiver chambers: insulin donor concentration was 100 nM (A) and 83·3 μM (B).

References

Arrigo, A. P., Tanaka, K., Goldberg, A. L., Welch, W. J. (1988) Identity of the 19S 'prosome' particle with the large multifunctional protease complex of mammalian cells. Nature 331: 192–194

Bai, J. P. F., Chang, L. L. (1995) Improvement of transepithelial transport of insulin: I. Insulin degradation by insulin-degrading enzyme in small intestinal epithelium. Pharm. Res. 12: 1171–1175

Bendayan, M., Ziv, E., Ben, S. R., Bar, O. H., Kidron, M. (1990) Morpho-cytochemical and biochemical evidence for insulin absorption by the rat ileal epithelium. Diabetologia 33: 197–204

Bendayan, M., Ziv, E., Gingras, D., Ben, S. R., Bar, O. H., Kidron, M. (1994) Biochemical and morpho-cytochemical evidence for the intestinal absorption of insulin in control and diabetic rats. Comparison between the effectiveness of duodenal and colon mucosa. Diabetologia 37: 119–126

Chang, L. L., Bai, J. P. F. (1994) Cellular enzymatic barrier to insulin absorption in rat small intestine and colon. AAPS(9) S: 302

Chiang, H. L., Dice, J. F. (1988) Peptide sequences that target proteins for enhanced degradation during serum withdrawal. J. Biol. Chem. 263: 6797–6805

Derewenda, U., Derewenda, Z. S., Dodson, G. G., Hubbard, R. E. (1990) Insulin structure. In: Cuatrecasas, P., Jacobs, S. (eds), Insulin. Springer, Berlin

Donowitz, M., Asarkof, N. (1982) Calcium dependence of basal electrolyte transport in rabbit ileum. Am. J. Physiol. 243: G28–G35

Duckworth, W. C. (1988) Insulin degradation: mechanisms, products, and significance. Endocr. Rev. 9: 319–345

Goldman J., Carpenter F. H. (1974) Zinc binding, circular dichroism, and equilibrium sedimentation studies on insulin (bovine) and several of its derivatives. Biochem. 13: 4566–4574

Jochen, A., Hays, J., Lee, M. (1989) Kinetics of insulin internalization and processing in adipocytes: effects of insulin concentration. J. Cell. Physiol. 141: 527–534

Kim, M. H., Curtis, G. H., Hardin, J. A., Gall, D. G. (1994) Transport of bovine serum albumin across rat jejunum: role of the enteric nervous system. Am. J. Physiol. 266: G186–G193

McClain, D. A., Olefsky, J. M. (1988) Evidence for two independent pathways of insulin-receptor internalization in hepatocytes and hepatoma cells. Diabetes 37: 806–815

Moss, A., Ward, W. F. (1991) Multiple pathways for ligand internalization in rat hepatocytes II: effects of hyperosmolarity and contribution of fluid-phase endocytosis. J. Cell. Physiol. 149: 319–323

Murakami, M., Takada, K., Fuji, T., Muranishi, S. (1988) Intestinal absorption enhanced by unsaturated fatty acids: inhibitory effect of sulfhydryl modifiers. Biochim. Biophys. Acta 939: 238–246

Quadros, E., Landzert, N. M., LeRoy, S., Gasparini, F., Worosila, G. (1994) Colonic absorption of insulin-like growth factor I in-vitro. Pharm. Res. 11: 226–230

Roth, R. A., Mesirow, M. L., Cassell, D. J., Yokono K., Baba, S. (1985) Characterization of an insulin-degrading enzyme from cultured human lymphocytes. Diabetes Res. Clin. Pract. 1: 31–39

Schilling, R. J., Mitra, A. K. (1990) Intestinal mucosal transport of insulin. Int. J. Pharm. 62: 53–64

Shiga, M., Hayashi, M., Horie, T., Awazu, S. (1987) Differences in the promotion mechanism of the colonic absorption of antipyrine, phenol red and cefmetazole. J. Pharm. Pharmacol. 39: 118–123

Sonne, O. (1985) Receptor-mediated degradation and internalization of insulin in the adenocarcinoma cell line HT-29 from human colon. Mol. Endocrinol. 39: 39–48

Sonne, O. (1988) Receptor-mediated endocytosis and degradation of insulin. Physiol. Rev. 68: 1129–1196

Sonne, O., Gliemann, J. (1983) The mechanism of receptor-mediated degradation of insulin in isolated rat adipocytes; indirect evidence for a non-lysosomal pathway. Mol. Cell. Endocrinol. 31: 315–331

Tsuji, A., Kurachi, K. (1989) Isolation and characterization of a novel large protease accumulated in mammalian cells in the presence of inhibitors. J. Biol. Chem. 264: 16093–16099